Hindawi
Geofluids
Volume 2021, Article ID 6623816, 18 pages
https://doi.org/10.1155/2021/6623816

Research Article

Seepage Analysis for Construction, with Applications to Some Projects in Hong Kong

Y. M. Cheng, Fu Chen, Zhen Zhu, Changfeng Yuan, and Liang Li

School of Civil Engineering, Qingdao University of Technology, Qingdao, China

Correspondence should be addressed to Zhen Zhu; zhuzhen@qut.edu.cn and Liang Li; liliang@qut.edu.cn

Received 24 December 2020; Revised 16 January 2021; Accepted 1 February 2021; Published 13 February 2021

Academic Editor: Feng Xiong

Copyright © 2021 Y. M. Cheng et al. This is an open access article distributed under the Creative Commons Attribution License, which permits unrestricted use, distribution, and reproduction in any medium, provided the original work is properly cited.

Deep excavations are intensively carried out in many cities in China and other countries. One of the major loadings in such construction work is the water pressure, and great effort is required to assess the seepage problem and the corresponding water pressure on the retaining wall for a good design and construction. Different methods used for the seepage analysis are discussed in this paper through a series of projects in Hong Kong. Some interesting phenomena from the seepage analysis will also be discussed. Two large scale seepage field tests in Hong Kong are also used for the illustration of the back analysis in seepage problems which are seldom carried out. The comparative studies demonstrate that a realistic seepage analysis is very important for deep excavation works, but it was not seriously considered in the past.

1. Introduction

In Hong Kong, China, and many developed cities in the world, deep excavations are necessary for the building foundations, basements, mass transit, subways, and other construction works [1–5]. In fact, excavation and lateral support (ELS) works are one of the major construction activities in Hong Kong and China, and many engineers are working on the design and construction of different ELS works. Many support systems have also been developed for different ground conditions with different ground water control systems [6]. In general, an ELS design submission includes

(1) Lateral support system, e.g., sheet piles and diaphragm wall

(2) Strutting (or tie-back) layout

(3) Construction sequence

(4) Supporting geotechnical documents

(5) Ground water seepage analysis, control of ground water, and estimates of ground movements

(6) Assessment of the effects of excavation and dewatering on adjoining structures

(7) Monitoring proposal for the ground settlement and ground water level

Cheng has worked on the design and construction of many deep excavations in Hong Kong. For example, for the Sheung Wan MTR Concourse, which is a 35 m deep diaphragm wall excavation in very poor soil, the water level has to be controlled to at least 2 m below the formation level during construction. The actual amount of water table drawdown is around 35 m depth; hence, the maximum water pressure difference at the two sides of the diaphragm wall is about $35 \times 9.81 = 343$ kPa (if hydrostatic), which is about three times the soil active pressure. The loading from water is hence the greatest loading for the design of the MTR concourse. Without the consideration of seepage, 343 kPa hydrostatic water pressure should be designed for the diaphragm wall which is a very expensive design. The ground settlement for this project amounted to 350 mm, and about 50% of the settlement came from the changes in the pore water pressure. To control the ground settlement in such a

poor soil condition, recharge wells have been used to restore the water table outside the diaphragm wall to a reasonable level. A careful and yet safe analysis and design of the water pressure is hence very important for the deep ELS works.

Following the incompressible flow assumption of water seepage through soil, the governing differential equation for seepage [7–9] is given in many text books [10–13] as

$$K_x \frac{\partial^2 h}{\partial x^2} + K_y \frac{\partial^2 h}{\partial y^2} = 0. \quad (1)$$

In the equation, h is the total head (the sum of elevation head and pressure head in the Bernoulli theorem) with the velocity head ignored due to its insignificant contribution and K_x and K_y are the coefficients of permeability of the soil in the X and Y directions defined by the Darcy Law as

$$v_x = K_x \frac{\partial h}{\partial x}, v_y = K_y \frac{\partial h}{\partial y}, \quad (2)$$

where v_x and v_y are, respectively, the velocities of flow of water in the soil in the X and Y directions. It is possible that the principal directions of permeability may not align with the horizontal and vertical directions; hence, the X and Y can be considered as the local principal directions for general cases. Due to the deposition and gravity actions, it can be assumed that the principal directions of permeability align along the vertical and horizontal directions for many practical problems. Though numerical methods [14–17] can always be used to solve Equation (1), Equation (1) can be solved by the flownet construction or analytical method for simple cases, approximate method by method of fragment for rapid design in simple cases, and finite difference/boundary element method for homogeneous problems with relatively regular geometry or the finite element for general cases. The construction of flownet is well understood and will not be repeated here. Analytical solutions of the equation can be found for certain cases where the geometries of excavations involving impermeable walls are simple (the analytical formulae are usually obtained by using complex conformal analysis). For more general conditions, the use of finite difference and finite element method (through the Galerkin formulation) is used. Currently, the most famous finite difference seepage program is the Modflow which is an open source code, while many proprietary pre-/post processors are also available. The use of the finite element method is more popular as compared with the finite difference method, as the use of imaginary nodes can be avoided. More importantly, for nonhomogeneous problems with irregular geometry, the use of the finite difference method is very difficult, and a special trick is required at the interface between different material regions. Many commercial codes are available for finite element seepage analysis, and this will not be discussed here.

2. Use of Analytical Method

The seepage problem of a simple problem can be mapped to a regular domain by the use of a complex conforming method [13, 18], and the governing Laplace equation can be solved then. After the solution of the Laplace equation in a regular square (rectangular) domain, the results can be mapped back to the original problem. Some analytical equations have been developed in the literature, but very few of them are known to the engineers or even researchers. The authors would like to pick up two cases for the illustration of such analytical methods, as these methods appear to be unknown to most of the engineers and researchers.

2.1. Case 1: Impermeable Layer at Depth at Infinity. For the example in Figure 1, rockhead is assumed to be so deep that it can be assumed to be at a depth of infinity. The authors have checked that *no* textbook has ever provided the guideline on the construction of flownet for such a case. For the engineers, they will simply assume a finite depth to draw the flownet or carry out finite element analysis as an approximation. Bettess [19] originated the infinite element for such a condition, which is further extended by Honjo and Pokharel [20] and Cheng [21]. The boundary element method has the advantage for this case, as the infinite domain is simple for this method. Nevertheless, for simple engineering cases, the use of the analytical method is actually simpler for applications but is virtually not known to most engineers. For Figure 1, the water level at the downstream side is kept at a depth of 0.5 m (by pumping) below the excavation level. In Figure 1, T is at most measured to the ground level of the upstream side even if the water level is above ground level while H is measured to the water level on the upstream side, regardless whether the water level is above or below ground. So $T = H$ if the water level is below ground on the upstream side, otherwise $T < H$.

If the soil is homogeneous and isotropic where $K_x = K_y$, Equation (1) can be reduced to

$$\frac{\partial^2 h}{\partial x^2} + \frac{\partial^2 h}{\partial y^2} = 0. \quad (3)$$

Analytical solutions for Equation (3) with geometry have been derived and are listed in Azizi [22], and a design guideline has been prepared by Cheng (see HKIE [23]):

(i) Determine η from Equation (4) by trial and error process

$$\tan(\pi\eta) - \pi\eta = \frac{\pi d}{T}. \quad (4)$$

(ii) Determine h_F (head at F, the toe level of the wall) by the relation

$$h_F = \eta H, \quad (5)$$

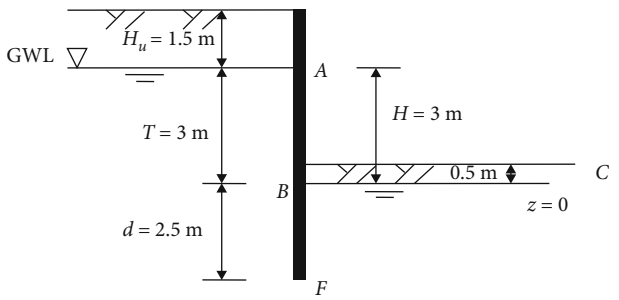

Figure 1: A seepage problem where the impermeable layer is found at a great depth.

$$\text{Determine } \lambda = \frac{H}{\pi}, \beta = \frac{T}{\pi}, \alpha = \frac{\beta}{\cos\left(h_F/\lambda\right)}. \tag{6}$$

(iii) The equation relating the total head h_z along the wall and depth z is

$$z = \frac{\beta h_z}{\lambda} - \alpha \sin \frac{h_z}{\lambda}, \tag{7}$$

where z is taken as zero at the downstream water level. It should be noted that the equation is applicable for both the upstream and downstream sides. When h_z increases along the flow from upstream to downstream, z will change from decreasing to increasing at the upstream course.

(iv) The average hydraulic gradient at the upstream side at the wall at level z is

$$i_{uz} = \frac{h_A - h_z}{T - z}, \tag{8}$$

where h_A is the total head at the ground surface of the upstream side.

The average hydraulic gradient at the upstream side at the wall at level z is

$$i_{ud} = \frac{h_z - h_B}{z}, \tag{9}$$

where h_B is the total head at the water surface of the downstream side.

(v) The actual pressure is $(h_z - z)\gamma_w$ where γ_w is the density of water.

For the problem in Figure 1, using Equations (4) to (7)

$$\begin{aligned} &\tan(\pi\eta) - \pi\eta = \frac{\pi d}{T} = \frac{\pi \times 2.5}{3} \Rightarrow \eta = 0.4209, \\ &h_F = \eta H = 0.4209 \times 3 = 1.2627, \\ &\lambda = \frac{H}{\pi} = \frac{3}{\pi} = 0.9549, \beta = \frac{T}{\pi} = \frac{3}{\pi} = 0.9549, \\ &\alpha = \frac{\beta}{\cos\left(h_F/\lambda\right)} = 3.8821. \end{aligned} \tag{10}$$

So the governing equation between z and h_z is

$$z = \frac{\beta h_z}{\lambda} - \alpha \sin \frac{h_z}{\lambda} = h_z - 3.882 \sin 1.0472 h_z. \tag{11}$$

The calculated results at the various levels on the upstream and downstream sides are tabulated in Table 1.

The calculated hydrostatic pressure profiles are plotted in Figure 2 as follows.

Based on the results in Table 1, the stability against the seepage force can be checked. For the design of the retaining wall, the net water pressure/force instead of the absolute value of the water pressure/force is used in the design. The results in Table 1 are plotted in Figure 2 against the hydrostatic pressure which are shown by the dotted lines. It is observed that for the upstream side, the water pressure drops below the hydrostatic value which is due to the release of the water for driving the water to move. On the other hand, the water pressure at the downstream side increases above the hydrostatic value due to the ingress of water. The total forces and moments on the wall due to the seeping water on both sides are summed and tabulated in Table 2.

With a factor of 1.5, the allowable average hydraulic gradient is $(19 - 10)/10/1.5 = 0.6$. The average hydraulic gradient at the downstream is 0.5 which is less than 0.6; the "quick sand" problem is hence checked to be acceptable. It should be pointed out that the water pressures at both sides of the wall toe must be equal, with a net water pressure of 0 at the toe of the retaining wall. For the Sheung Wan MTR Concourse, if hydrostatic pressure is applied, the design water pressure will be 343 kPa instead of 0 kPa at the toe of the retaining wall which is highly conservative! Thus, the adoption of the "no seepage" hydrostatic pressure for the design will be very conservative, but surprisingly, this issue is seldom addressed clearly in nearly all the existing textbooks. For some relatively shallow excavations, some engineers even assume hydrostatic water pressure for the design, which is obviously a waste of money.

For the present case, there is actually no need to draw the flownet, as the water pressure is sufficient for all the analyses and design of the problem. Concurrently, there is also no simple method to draw the flownet for this case.

2.2. Case 2: Impermeable Layer at Finite Depth. If the depth to rockhead is finite, an impermeable boundary has to be considered which is illustrated by the problem in Figure 3. This case is well illustrated in many textbooks which can be solved by the flownet construction.

The calculation procedures are shown in Figure 4. For the problem in Figure 3, $\xi = 1.0985$, $h_A = 1.7548$ m, and $h_B = -1.2452$ m. The heads, hydraulic gradients, and water pressures due to seepage are given in Table 3.

The calculated hydrostatic pressure profiles are plotted in Figure 5 as follows.

The total force and moments on the wall due to the seeping water on both sides are summarized in Table 4.

Compared with case 1, there is a slight increase in the forces and moments on the sheet pile wall. This result appears interesting and is not reported previously. Since such

Table 1: Summary of heads/pressures for case 1.

(a) Summary of upstream side				(b) Summary of downstream side			
Head h_z (m)	Depth z (m)	Average hydraulic gradient i_{zu}	Hydraulic pressure $(h_z - z)\gamma_w$ (kPa)	Head h_z (m)	Depth z (m)	Average hydraulic gradient i_{zd}	Hydraulic pressure $(h_z - z)\gamma_w$ (kPa)
3	3	0	0.00	0	0.0000	0	0.00
2.75	1.7452	0.1992	10.05	0.25	−0.7548	−0.3312	10.05
2.5	0.5589	0.2048	19.41	0.5	−1.4411	−0.3470	19.41
2.25	−0.4951	0.2146	27.45	0.75	−1.9951	−0.3759	27.45
2	−1.3620	0.2293	33.62	1	−2.3620	−0.4234	33.62
1.75	−1.9999	0.2500	37.50	1.25	−2.4999	−0.5000	37.50
1.625	−2.2239	0.2632	38.49	1.272	−2.5000	−0.5088	37.72
1.5	−2.3821	0.2787	38.82				
1.45	−2.4268	0.2856	38.77				
1.4	−2.4609	0.2930	38.61				
1.272	−2.5000	0.3142	37.72				

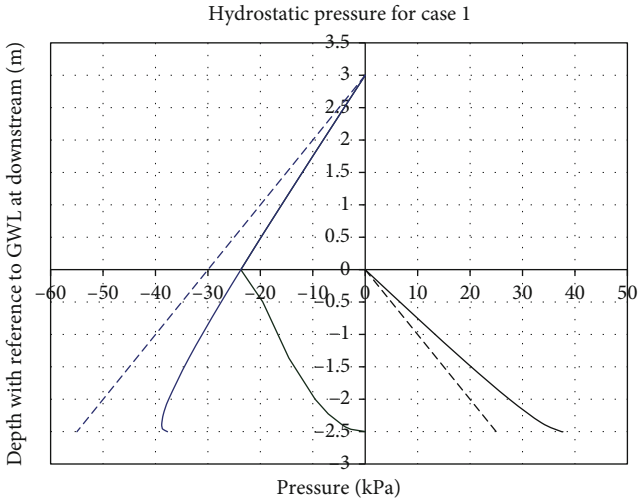

Figure 2: Hydrostatic pressures on the wall in Figure 1. Note that the dashed blue line (left 1) means the upstream water pressure on the wall stem without seepage, the real bold blue line (left 2) means the upstream water pressure on the wall stem with seepage, the real cyan line (left 3) means the net water pressure on wall stem with seepage, the dashed black line (left 4) means the downstream water pressure on wall stem without seepage, and the real bold black line (left 5) means the downstream water pressure on the wall stem with seepage.

Table 2: The total forces and moments on the wall for case 1.

Force (kN) per meter width			Moment (kNm) about wall toe per meter width		
Upstream	Downstream	Net	Upstream	Downstream	Net
116.8	42.99	73.81	218.33	35.19	183.14

increase is small, it can be considered that unless the rock-head is near to the toe of the sheet pile, the use of case 1 for normal design is already adequate. It should also be noted that for the water pressure above the formation level at the upstream side, the water pressure distribution is nearly a straight line even after the seepage, though the value is less than the hydrostatic value. This is observed for both cases 1 and 2.

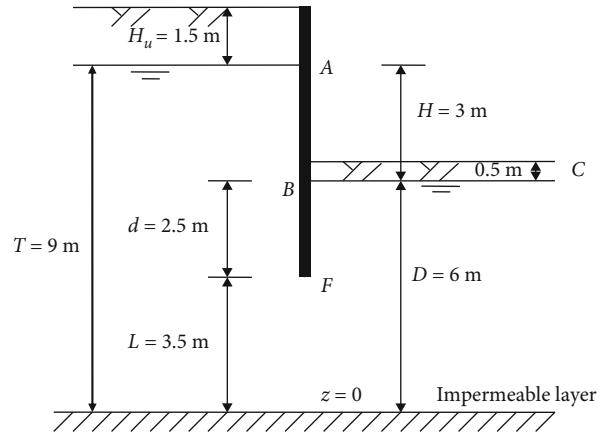

Figure 3: A seepage problem where the impermeable layer is found at limited great depth.

3. Finite Difference Method

The Laplace equation can be solved by means of the finite difference method, which is particularly appealing for three-dimensional problems where a large matrix is not required [24]. For case 2, the finite difference solution yields the total head contours (or equipotential lines) in Figure 6. A set of "flow lines" perpendicular to the total head contours is superimposed onto the total head contours to form the "flownet."

The "pressure head" can be obtained by subtracting the elevation head from the total head as determined previously. The pore water pressure can then be determined by multiplying the pressure head by the density of water, and the final results will be similar to that in Table 2.

If an impermeable layer exists at a great depth, it is required to assume an impermeable boundary with the finite difference method. On the contrary, an infinite element can be used for the finite element method for such condition. It can be concluded that the finite difference method is less

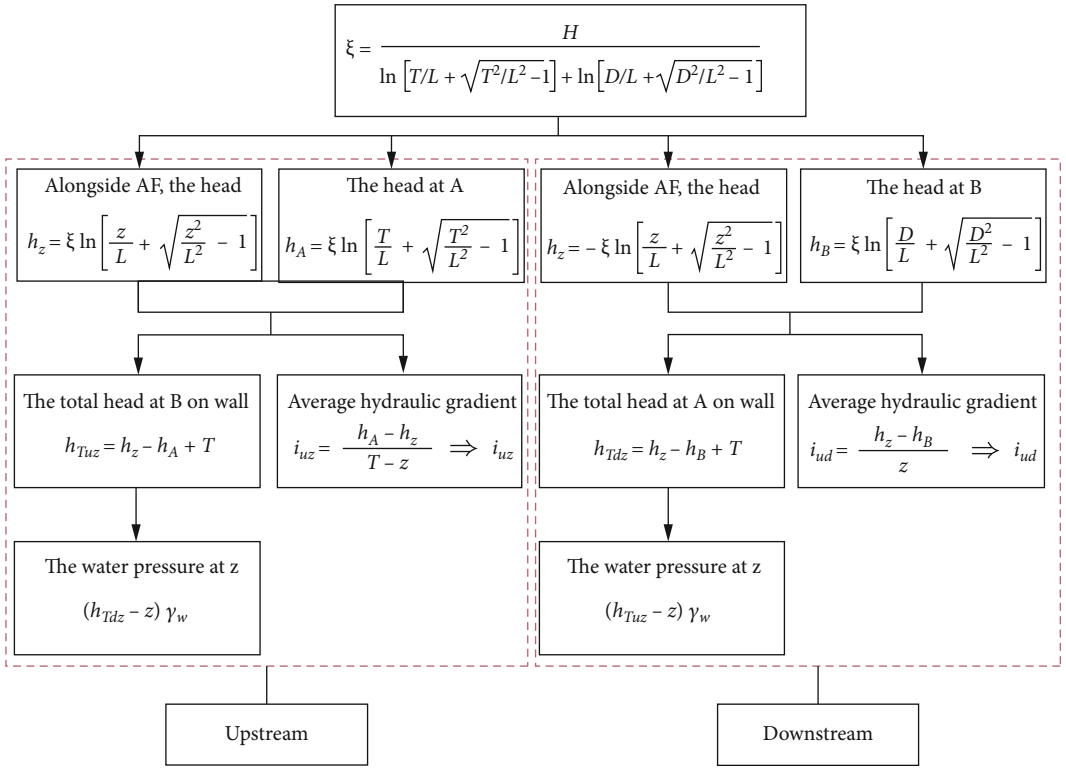

Figure 4: The flowchart for case 2.

versatile as compared with the finite element method. The use of the finite difference has an advantage over the finite element: the speed of computation. Finite difference analysis is much faster than the finite element analysis in terms of computer time, but this is not important for the modern computer where the CPU is fast enough.

4. Finite Element Approach

The seepage problem is best solved by the finite element method, where the Galerkin formulation is applied to form the element stiffness matrix $[K^e]$ as

$$[K^e] = \int\int [T]^T [k_c][T]dxdy, \tag{12}$$

where

$$k_c = \begin{bmatrix} k_x & 0 \\ 0 & k_y \end{bmatrix} [T] = \begin{bmatrix} \frac{\partial N_1}{\partial x} & \frac{\partial N_2}{\partial x} & \frac{\partial N_3}{\partial x} & \frac{\partial N_4}{\partial x} \\ \frac{\partial N_1}{\partial y} & \frac{\partial N_2}{\partial y} & \frac{\partial N_3}{\partial y} & \frac{\partial N_4}{\partial y} \end{bmatrix}. \tag{13}$$

N_i are the interpolation functions for a quadrilateral element. For three nodes or higher order elements, the matrix size for $[T]$ in Equation (13) will be modified accordingly. Very detailed treatment of this problem is given by Smith et al. [25], Asadzadeh [26] and many others, and sample coding in Fortran 90 has been developed by Cheng which can be obtained at natureymc@yahoo.com.hk. If the principal directions of the permeabilities are not the global x and y directions, the coordinates of the element can be rotated to the local principal directions x' and y' axes. The "stiffness matrix" can be formed by using the transformed coordinates while the element stiffness matrix $[K^e]$ is not required to be modified. This is possible as the degrees of freedom are only the total head which are independent of the coordinate axes.

For illustration, the seepage analysis for the project Kwun Tong Line Extension-Whampoa Station in Hong Kong is given in Figure 7.

For the West Rail Tsuen Wan West Station project, the site is mainly underlain by sandy/silty material comprising the fill, alluvium, and completely to highly decomposed granodiorite layers; elastic settlement will generally be induced as a result of dewatering. This is assessed by applying the effective stress change to the soil stratum down to the top of the stiff material (i.e., completely to highly decomposed tuff layer). With reference to the current monitoring record, it was noted that the lowest groundwater table of SP1 (at the southeast side of the site) is recorded to be +1.79 mPD. Therefore, in the analysis, the groundwater level is taken at +1.79 mPD for the southeast side of the construction site and +2.1 mPD for the other remaining sides of the site based on the monitoring record during construction. The seepage analysis for this project is shown in Figure 8. The monitoring record for piezometer SP1, the results of the SEEP/W analysis, and the induced ground settlement are estimated. The maximum settlement due to the groundwater drawdown is estimated to be -6.07 mm. Pump wells and observation wells are installed along the critical sections for pumping tests.

Table 3: Summary of heads/pressures for the problem in Figure 3.

(a) Summary of upstream side					(b) Summary of downstream side				
Depth z (m)	Head h_z (m)	$h_{Tuz} = h_z - h_A + T$ (m)	Average hydraulic gradient i_{zu}	Water pressure $(h_{Tuz} - z)$ γ_w (kPa)	Depth z (m)	Head h_z (m)	$h_{Tdz} = h_z - h_B + D$ (m)	Average hydraulic gradient i_{zd}	Water pressure $(h_{Tdz} - z)\gamma_w$ (kPa)
9	1.7548	9.0000	0.0000	0.00	6	−1.2452	6.0000	0.0000	0.00
8.5	1.6863	8.9315	0.1370	4.31	5.5	−1.1246	6.1206	−0.2412	6.21
8	1.6127	8.8579	0.1421	8.58	5	−0.9838	6.2614	−0.2614	12.61
7.5	1.5332	8.7784	0.1477	12.78	4.5	−0.8118	6.4334	−0.2889	19.33
7	1.4467	8.6919	0.1541	16.92	4	−0.5804	6.6648	−0.3324	26.65
6.5	1.3514	8.5966	0.1614	20.97	3.5	0.0000	7.2452	−0.4981	37.45
6	1.2452	8.4904	0.1699	24.90					
5.5	1.1246	8.3698	0.1801	28.70					
5	0.9838	8.2290	0.1927	32.29					
4.5	0.8118	8.0570	0.2096	35.57					
4	0.5804	7.8256	0.2349	38.26					
3.5	0.0000	7.2452	0.3191	37.45					

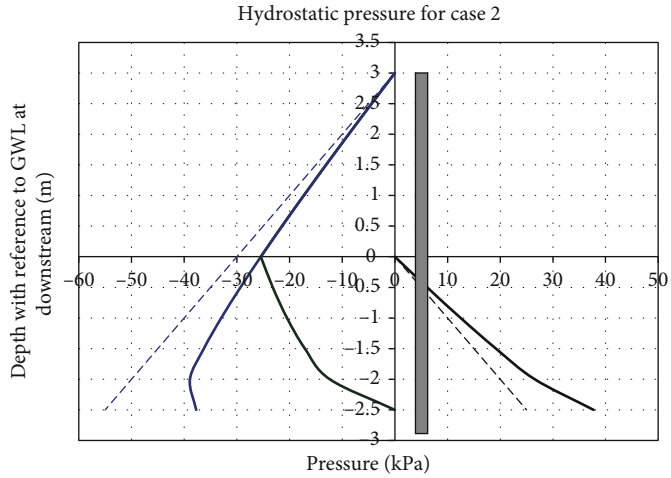

Figure 5: Hydrostatic pressures on the wall for the problem in Figure 3. Summing the total force and moments on the wall due to the seeping water on b. Note that the dashed blue line (left 1) means the upstream water pressure on the wall stem without seepage, the real bold blue line (left 2) means the upstream water pressure on wall stem with seepage, the real cyan line (left 3) means the net water pressure on the wall stem with seepage, the dashed black line (left 4) means the downstream water pressure on the wall stem without seepage, and the real bold black line (left 5) means the downstream water pressure on the wall stem with seepage.

Table 4: The total forces and moments on the wall for case 2.

Force (kN) per meter width			Moment (kNm) about wall toe per meter width		
Upstream	Downstream	Net	Upstream	Downstream	Net
121.0	41.76	79.24	229.67	33.56	196.12

5. Unconfined Flow

Based on the observations on many deep excavation projects in Hong Kong, Shenzhen, and other places, the authors have noted that the assumption of prescribed constant ground water level on the upstream side which is assumed in nearly all the textbooks is not an appropriate assumption. The water level outside the retaining wall actually falls during construction, which results in "unconfined flow" where the upstream profile becomes another unknown to be solved. In fact, ground water control is an important issue for deep excavation analysis, and many methods have been developed to control the ground water during excavation [27–29]. For Cheng's past experience, recharge wells outside the retaining wall have been used to restore the water table for the Sheung Wan and Wanchai MTR Concourses in Hong Kong.

The free surface is governed by $\phi = y$ ($u = 0$) and flow rate normal to the free surface being 0. Consideration of free surface flow is commonly neglected by many engineers in the routine analysis and design. Consider the boundary conditions for a typical seepage problem as shown in Figure 9. If the boundary condition along AB is a constant head, that will be a classical seepage problem, and the water table along AG will remain stationary during seepage analysis. If the total head along AB is assumed to be varying with the boundary condition $\phi = y$ along AG (also no flow across AG), then the precise position of AG will be an unknown which can be determined from iterative finite element analysis.

In the finite element analysis, there are two major approaches towards this problem. In the first approach, the mesh will deform while the number of elements remains unchanged until the domain satisfies all the boundary conditions. The first approach which is an adaptive mesh method is useful when the trial free surface is not significantly different from the true free surface. This method is simple to be implemented, yet there are many disadvantages which are as follows:

(1) The elimination of the dry soil domain prohibits concurrent calculation of the deformation of the soil structure

(2) The use of this method may lead to poor results or even divergence because the mesh may be highly distorted during the iteration process. This problem will be extremely prominent at the interfaces of materials with large differences in permeabilities

(3) The number of iterations and the total solution time required for solution are generally great

In the second approach, some of the nodes outside the valid domain (with negative water pressure) will be removed until no more nodes can be removed. The mesh will then slightly deform to fine tune the satisfaction of all the boundary conditions. This approach will involve nodes and element renumbering which can be tedious work. The second approach can avoid some of the disadvantages of the first approach as mentioned above. The use of the Baiocchi transformation [30] can lead to the existence theorem, but it is not general enough to be implemented for the nonhomogeneous medium with arbitrary geometry. Residual flow procedure is the most common method that is used for the second approach, and many variations on this procedure have been developed. A simple method for the implementation of this approach can be achieved by the use of "air element" used for the modelling of excavation process as proposed by Desai. Under this concept, any element which is "inactive" in the

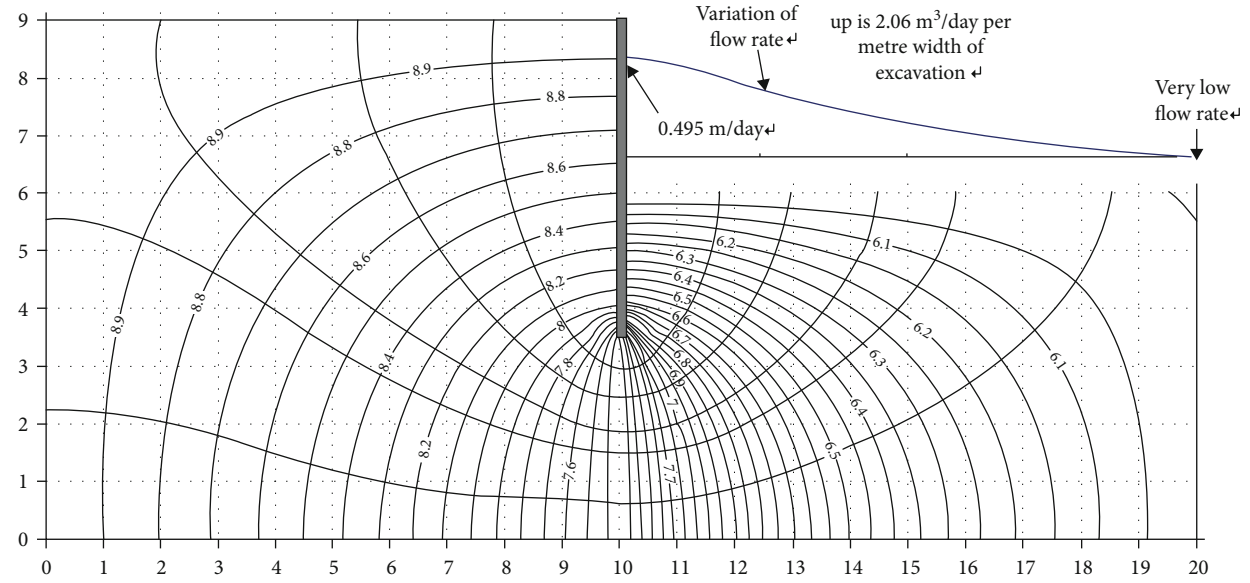

Figure 6: Flownet for case 2 by the finite difference method.

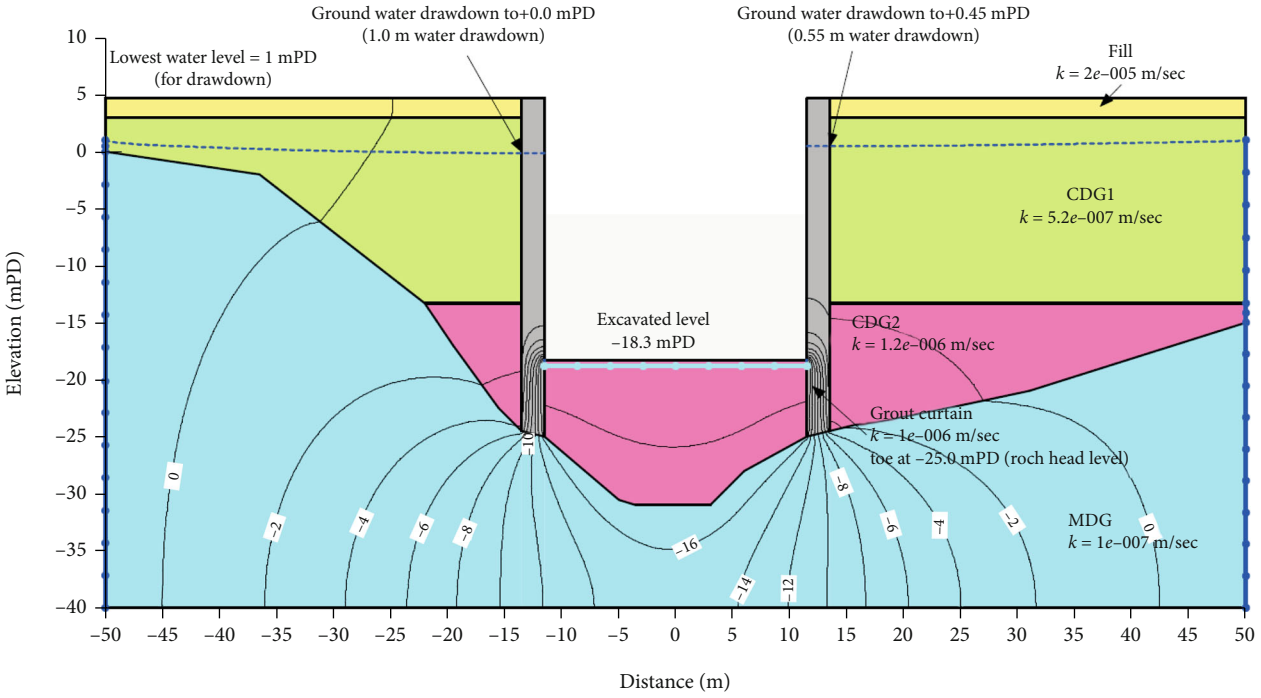

Figure 7: Seepage analysis for the Kwun Tong Line Extension-Whampoa Station in Hong Kong by finite element method.

analysis will be given a small but finite permeability/stiffness. Since the stiffness of the "air element" is much smaller than the remaining elements, its effects on the iteration analysis will be negligible. Complicated computer coding can then be avoided because the computations are carried out on a mesh which remains unchanged. Bathe has proposed a simple solution method which is based on this concept. Either the Newton-Raphson or modified Newton-Raphson solution method is usually employed for the analysis. The Newton-Raphson method is preferred if the active zone differs significantly from the original finite element mesh. The disadvantages of these commonly used methods are as follows:

(1) The stiffness of the air element is finite but small; hence, the spectral condition number associated with the system stiffness matrix will be large. The solution error will be great unless a double precision computation is used in the computation. It is suggested by Ridlon [31] that the difference in the stiffness of adjoining element should preferably be not greater

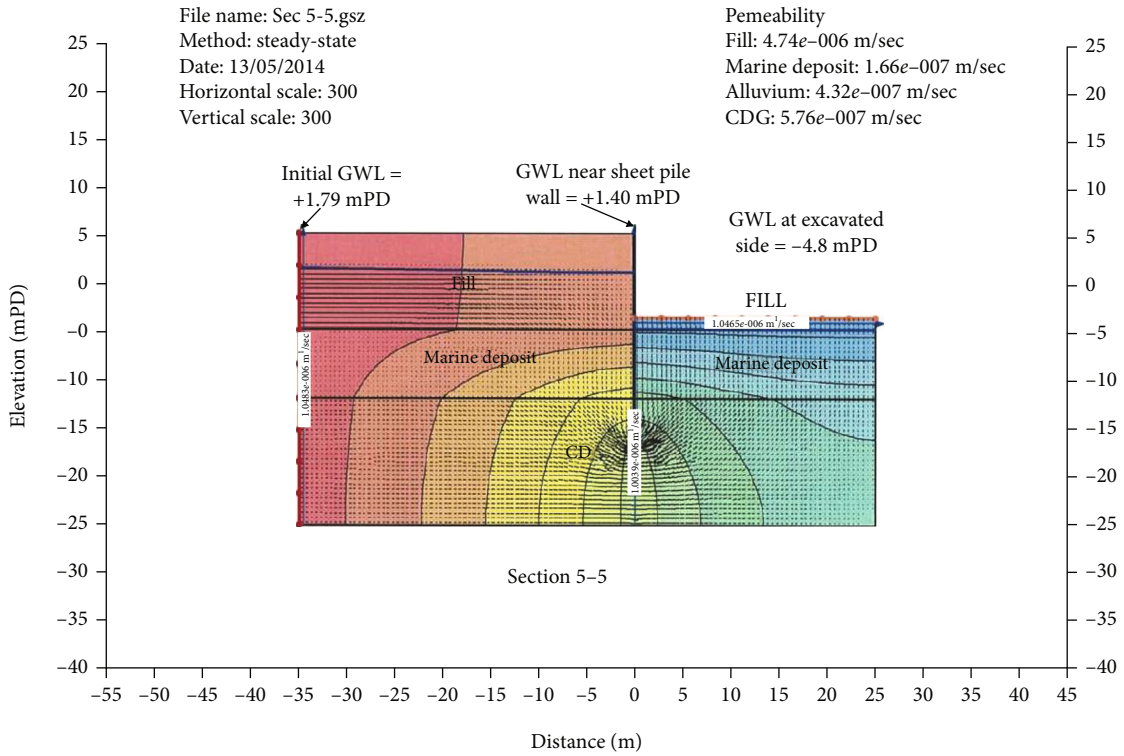

Figure 8: Seepage analysis for the West Rail Tsuen Wan West Station in Hong Kong.

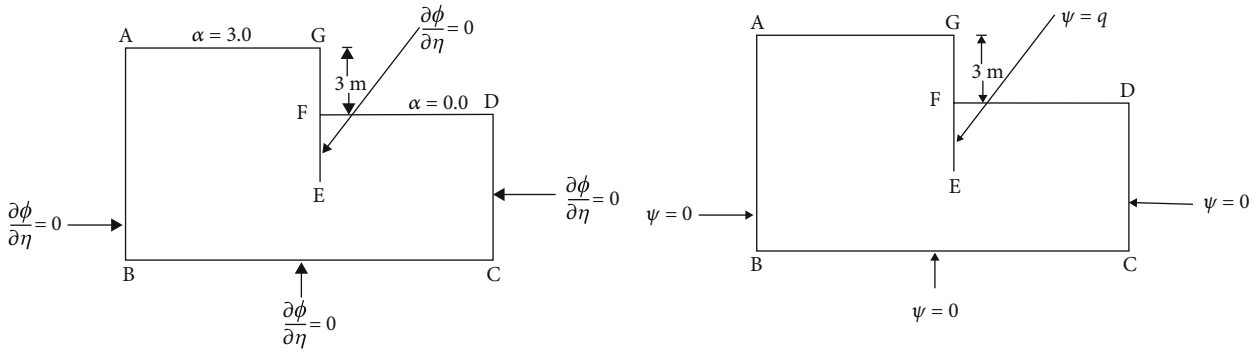

(a) Solution for the total head

(b) Solution for the stream function

Figure 9: Boundary condition for a seepage problem.

than 10000 times for most problems in order to minimize the solution error

(2) Unnecessary computations are required for the elements and nodes which are outside the free surface

(3) Complicated procedures are used for the evaluation of the equivalent forces during iteration

(4) The method of penalty is used for the nonlinear iteration analysis or the modelling of the flow exits through the downstream boundary. This will also induce solution error in the analysis

Cheng and Tsui [32] proposed a modified approach for approach two, where the nodes to be removed will remain in the mesh while the elements outside the valid domain will not be considered in the element stiffness matrix. The global stiffness matrix will still be based on the original mesh, but the total head of the "air nodes" will be prescribed as 0. Thus, all the "air nodes" will be prescribed nodes, with a result that there is no need to renumber the nodes and element. The precise domain will then be obtained by an interpolation process which is good enough for normal purposes, unless very few elements are used for the analysis. This approach appears to be superior to the classical approach two because it is simple in operation and fast in computation.

One of the difficult problems for the free surface seepage analysis is the radius of influence R_0, which is largely empirical. Currently, this value is usually taken from statistical

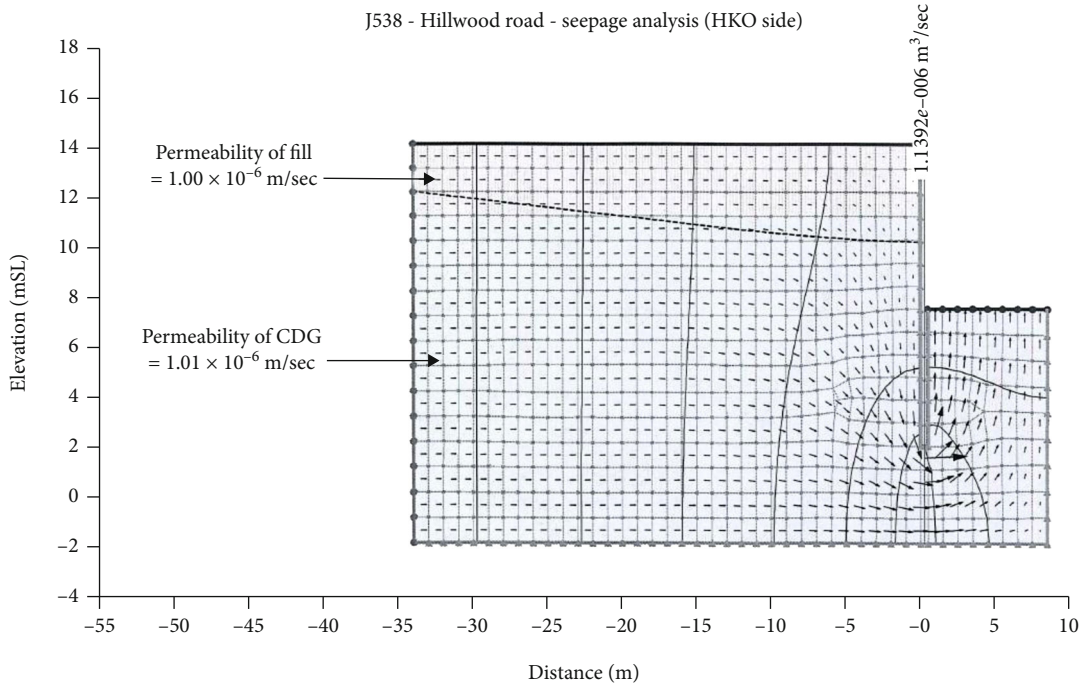

Figure 10: Hillwood Road free surface seepage flow by the use of true air element by Cheng.

information. Alternatively, a simplified method is adopted by some engineers as

$$R_0 = CH\sqrt{k}, \tag{14}$$

where C is a constant, H is the amount of drawdown, and k is the permeability of soil as determined from field test. C is commonly taken as 3000 for radial flow and 1500 for line flow to trenches or well points. In Hong Kong and many other countries, the radius of influence is also commonly taken as twice the depth of excavation, and this is generally sufficient for design purposes. For large scale construction problems, the radius of influence can be determined by field tests, but this is seldom carried out in practice.

For the problem in Figure 9, the finite element equation will be $[K]\{\phi\} = \{q\}$, where $\{q\}$ is the vector of point source or sink. For a steady state problem where the head is prescribed along AG and FD, this matrix equation can be solved directly to give ϕ. If AG is assumed to be a free surface, then the boundary condition of AB is given as ϕ = constant and given by height AB, while the precise location of AG will be varied until $\phi = y$ and $u = 0$ along AG.

While most of the engineers, design charts, and figures are based on the assumption that the water table outside the excavation remains stationary, Cheng has observed that this assumption is not valid. For the Mass Transit Railway construction in Hong Kong, Cheng has analyzed many water drawdown measurement results, and significant drawdown can be possible for many projects. In fact, the recharge well is used to restore the water table outside the excavation to control the ground settlement arising from the construction. In Figure 10, an example of free surface flow analysis using the true air element by Cheng is carried out for the project at Hillwood Road, Hong Kong. It should be noted that free surface flow analysis for excavation work is seldom carried out for normal engineering works, as most of the engineers are not aware of the importance of free surface flow. The drop in the water level outside the retaining wall is very significant as shown in Figure 10, and this should not be neglected in the analysis and design.

6. Water Pressure Difference

Based on the finite element/difference method or equivalently flownet construction or the free surface construction, the net water pressure difference at the retaining wall for ELS can be illustrated in Figure 11. In general, the actual water pressures at the two sides of the retaining wall are not required, and the net water pressure difference will be sufficient for the analysis and design of the ELS. As shown in Figure 11, the net water pressure difference from finite element/flownet is nearly a triangular distribution, except at the tip of the sheet pile where there is a very rapid change of the water pressure. This result is similar between the classical confined flow and the free surface flow analysis. The blue line in Figure 11 is based on the free surface flow analysis which is actually observed in many deep excavation works by Cheng, and the water pressure is smaller than the classical approach where the water table outside the retaining wall remains stationary during construction. A simplified approach is adopted in Hong Kong (see also Ou [33]), where

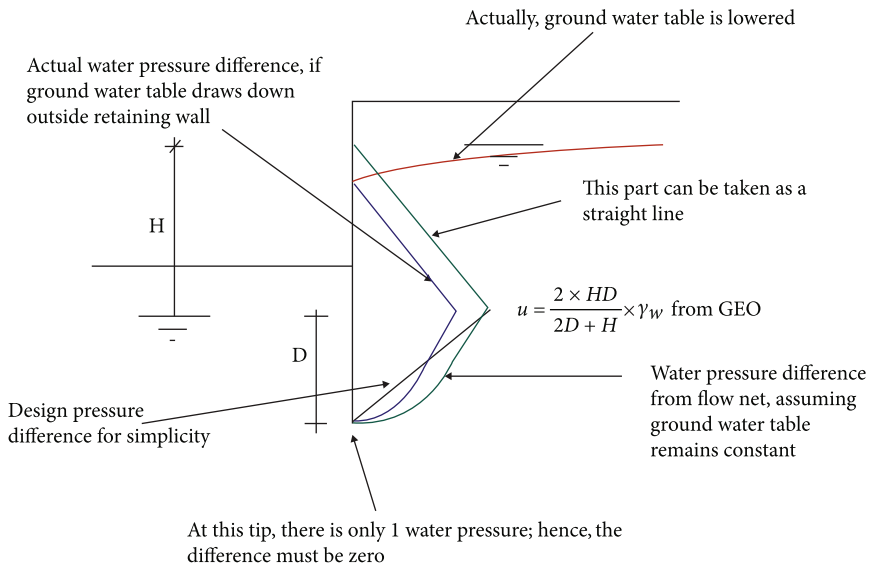

Figure 11: Design net water pressure difference on the retaining wall.

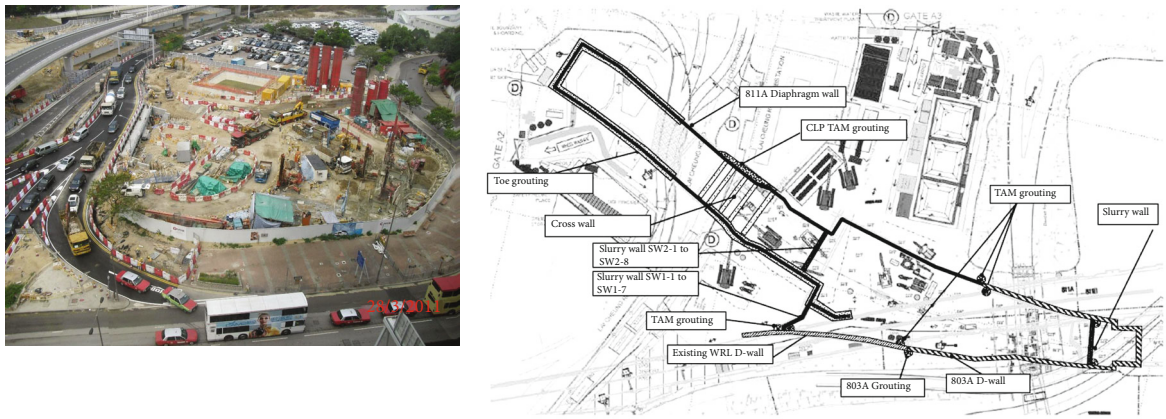

(a) (b)

Figure 12: XRL site at Hoi Ting Rd. and WRL Tunnel, with 300 m long cofferdam made of diaphragm wall: (a) site photo before construction; (b) locations of diaphragm wall, slurry wall, and toe grouting prior pumping test.

the design water pressure difference is a triangular pressure, and the maximum water pressure is given by

$$u = \frac{2 \times HD}{2D + H} \times \gamma_W. \quad (15)$$

It should be mentioned that the net water pressure difference at the tip of the retaining wall must be zero. Cheng has been asked by many engineers and students about this, as a trapezoidal water pressure difference assuming hydrostatic condition is used by many engineers in the actual design. At any point, there is only one water pressure; hence the net water pressure difference at the tip of the sheet pile must be zero, but this simple fact has been neglected by some engineers. Again, the importance of the actual water pressure difference across a retaining wall as indicated in Figure 11 is not noticed by many engineers and researchers. The illustration in Figure 11 also appears to be unique which is absent in all the textbooks that the authors have checked.

7. Field Tests for Guangzhou-Shenzhen-Hong Kong Express Rail Link (XRL) Project and West Kowloon Reclamation Project

The permeabilities of soil obtained from laboratory tests are well known to be several times smaller than the in situ permeability. For large construction projects where the amount of water table drawdown is significant, good estimates of the permeabilities of soils are important, but this is usually not carefully considered in actual construction. The authors would like to discuss two major projects in Hong Kong, where extensive drawdown seepage tests are carried out. For the first project, the Guangzhou-Shenzhen-Hong Kong Express Rail Link (XRL) (Figures 12 and 13), it is an express rail link connecting Hong Kong, Shenzhen, and Guangzhou.

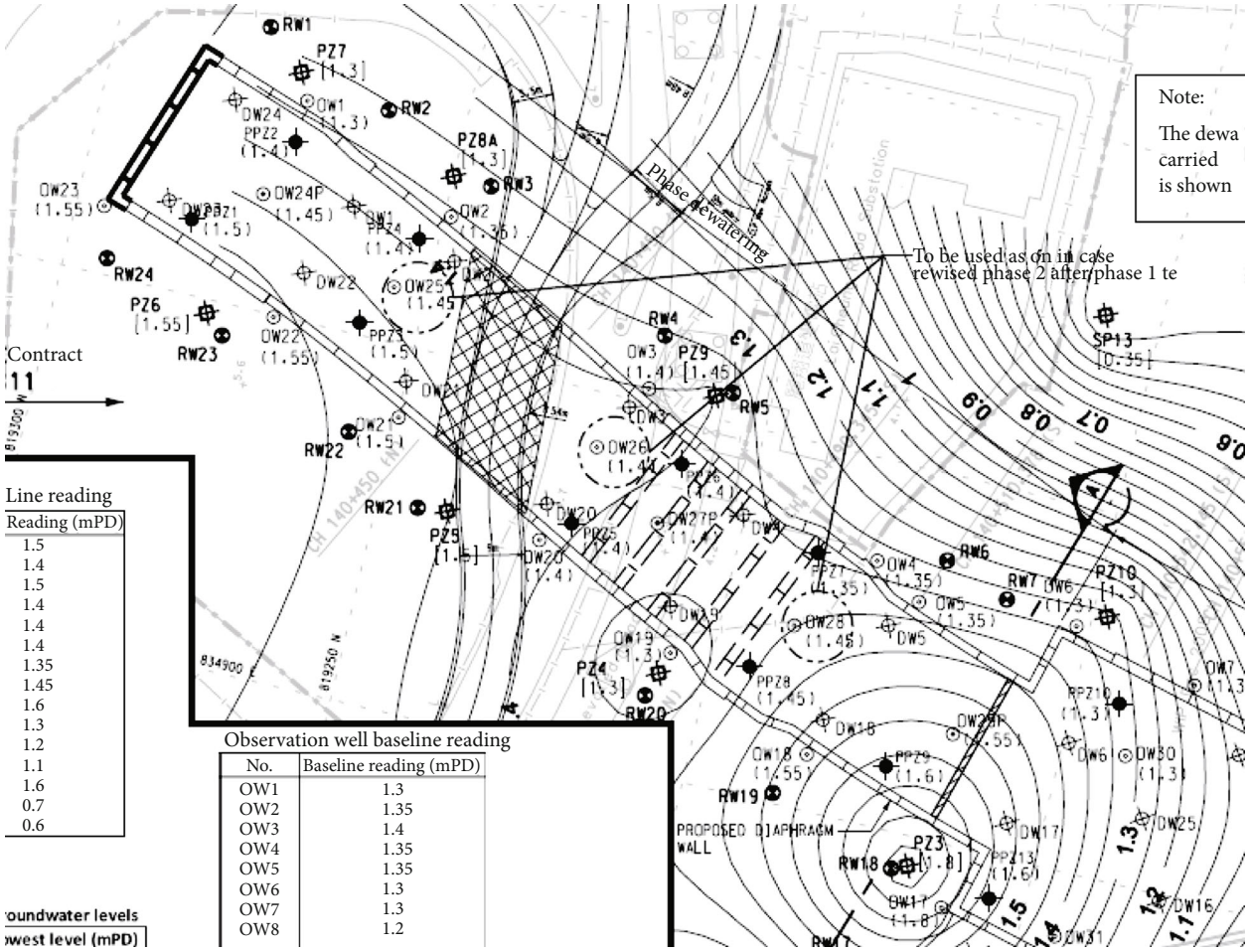

Figure 13: Locations of recharge wells.

It is aimed at providing a fast and convenient railway service linking the three places. The Hong Kong section of the XRL will be a 26 km long underground rail line on a dedicated track that runs from the terminus in West Kowloon to the boundary at Huanggang, where it will connect with the XRL Mainland section. Prior to commencing the bulk excavation for the tunnel, pumping tests were carried out first to verify the actual permeabilities of the soil and to carry out the design for the dewatering system. Different types of underground soil with different characteristics such as permeability (K value) will generate different test results, and the permeability and pore pressure distribution will be determined in this project.

The main purposes of the pumping tests are to prove the effectiveness of the cofferdam waterproofing prior starting any main excavation work and to estimate the permeabilities of different types of soils and to check the effects of dewatering on the existing adjacent structures prior starting any main excavation work. Due to different construction progress and achievement, the contractor will separate the pumping tests into 3 sections, i.e., (1) the northern section (July 2011), (2) the southern section (August 2011), and (3) the 811B interface section (May 2012).

Dewatering procedure in each section will be conducted in 2 stages. An intermediate stage of pumping test for dewatering to -9.3 mPD will be carried out prior to proceeding to the final stage of the pumping test to -24.4 mPD. This sequence of dewatering will allow the later construction of ELS in 2 distinct parts. Hence, the contractor will conduct a total of 6 independent dewatering stages (2 stages for each of the 3 different sections). A number of instruments to monitor the dewatering are being installed.

There are 4 types of wells which are being used on site:

(1) *Dewatering wells*: those wells will provide sufficient dewatering capacity to lower down the ground water table (GWT) inside the cofferdam

(2) *Observation wells*: those wells will measure the GWT level inside and/or outside the cofferdam

(3) *Observation wells including piezometer*: those wells will allow the contractor to know the GWT level below the layer of the marine deposit

(4) *Recharge wells*: those wells act as contingency measures to keep the GWT level outside the cofferdam to a definite level

The test for the northern section was carried out in the middle of June 2011, while the test for the southern one

Table 5: Layout of dewatering monitoring.

	Northern section
Dewatering well	12 nos.: DW1, DW2, DW3, DW4, DW5, DW18, DW19, DW20, DW21, DW22, DW23, DW24 +DW6 & DW17 (as observation well)
Observation well	13 nos.: OW1, OW2, OW3, OW4, OW5, OW6, OW17, OW18, OW19, OW20, OW21, OW22, OW23
Observation well including piezometers	3 nos.: OW24P, OW27P, OW29P
Observation well used as reserved dewatering well	3 nos.: OW25, OW26, OW28
Recharge well	15 nos.: RW1, RW2, RW3, RW4, RW5, RW6, RW7, RW17, RW18, RW19, RW20, RW21, RW22, RW23, RW24

Table 6: Pumping test monitoring frequency.

Pumping test criterion Reading frequency	Dewatering well reading frequency	Observation well reading frequency		Piezometer reading frequency	
	Inside	Inside	Outside	Inside	Outside
Readings to be measured during 7 days prior pumping test starting	4 hrs	4 hrs	4 hrs	Hourly	Daily

was carried out in the middle of July. Both the northern and southern sections contained 3 types of wells: dewatering well, observation well, and recharge well. For each of them, a number of instruments to monitor dewatering are being installed (see Table 5).

7.1. Pump Test Procedure and Sequence

7.1.1. Outline Requirements. The contractor has planned to conduct the pumping test over 3 sections separated by a slurry wall connecting panels AT-WE18 to AT-WW18, and a D-wall connecting panels AT-WW41 to the existing WRL tunnel.

7.1.2. Ground Water Table Baseline. Prior to commencing any pumping tests, the contractor will provide a unique GWT baseline for all types of instruments: For instruments outside the cofferdam with a long reading story, the contractor will take into consideration the readings of the last 10 months with available instruments (piezometers, standpipe). For the recent installed instruments inside and outside the cofferdam, the contractor will monitor the instruments for 7 days at a frequency shown in Table 6. The values will be compared with the 10-month readings and corrected where required.

The GWT baseline will be established by considering the lowest water level recorded.

7.1.3. Equipment Test. To avoid any failure in the dewatering procedure due to material malfunction, the contractor will ensure that all installed plant and materials are working properly prior to the pumping test. Each of the above equipment will be checked thoroughly following a checklist previously agreed by the engineer:

(1) Each type of well (vertical tubes, pumps, riser pipe, float switch, and filter material)

(2) Pipe lines (setting-out, seepage at valve, and float switch)

(3) Flow meters and pressure gauges

(4) Instrumentation (through a damage instrument list in daily reports)

(5) Plants and tank (permit to work and license)

If an observation and/or recharge well is found to be malfunctioning during the pumping test, the well will be flushed and a response test will be performed to ensure that the well is working properly. The individual elements of the system will be checked prior to installation. The on/off switches will be inspected and checked for function in water. The pump will be switch on prior to installation and checked for flow capacity by lowering into the well and monitoring the water volume over time. Any pump that fails to activate during a pumping test will be deemed to be malfunctioning and will be immediately replaced. If the water level goes below the switch off level or above the switch on level and the pump fails to respond, then the on/off switches will be deemed to be malfunctioning. In this case, the pump will be controlled manually using the water levels measured from the piezometer installed inside the pump well.

7.1.4. Constant Discharge Test. After completion of the equipment test, the dewatering test can commence (Figures 14, 15, 16, and 17). As a 10-meter layer of marine deposit will be encountered during the pumping test, the designer has decided to separate the pumping test into 2 phases:

(1) *Phase 1*: dewatering to -9.3 mPD

(2) *Phase 2*: dewatering to -24.4 mPD

The 2-stage operation will allow the contractor to construct the three upper levels of struts which will be carried

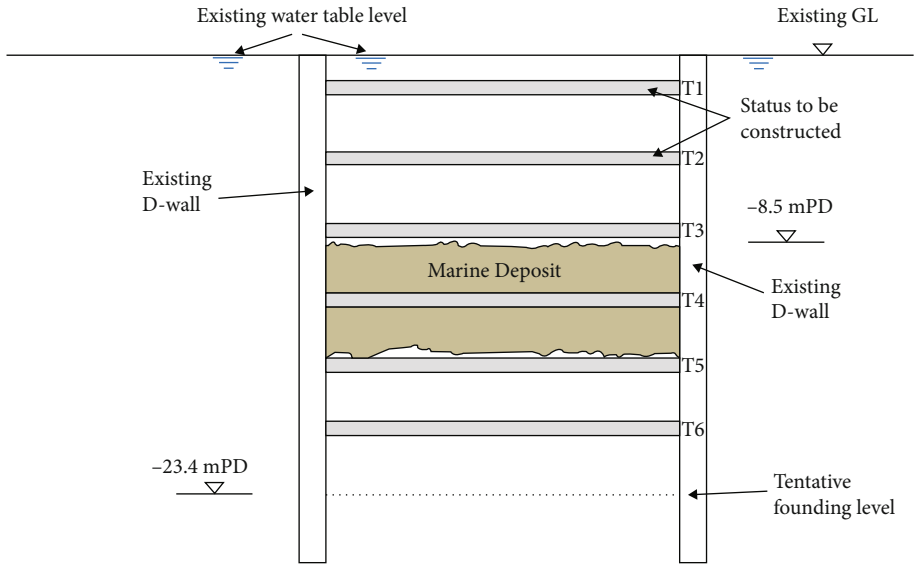

Figure 14: Initial condition prior staring pumping tests.

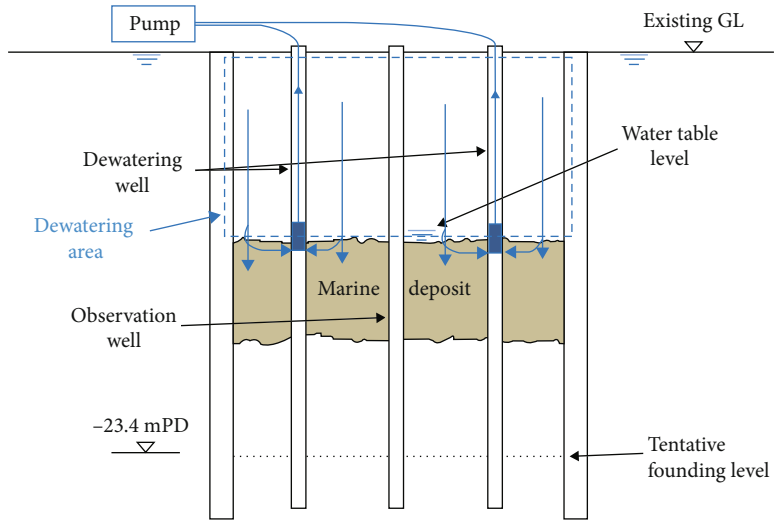

Figure 15: Pumping Tests, stage 1.

out at the same time together with required additional remedial works on the lower part of the D-wall. It will save a considerable amount of time as 2 types of works will be carried out at the same time but independently in technical matters. Wells will be pumped continuously at a defined flow previously agreed by the designer. At a certain point of pumping, the steady rate of discharge with the required drawdown is achieved. Steady state is defined as the constant rate of pumping such as the rate of groundwater both inside and outside the diaphragm wall shaft measured in the observation wells and piezometers as less than 0.1 m per hour over three successive hourly readings. Steady rate shall be defined as the constant rate of groundwater drawdown both inside and outside the site which is less than 0.1 m over an hour. The minimum test period shall be 7 days. However, if the contractor maintained the steady state for 72 consecutive hours, subject to approval of the engineer, the test period may be shortened. Where the steady state will not be reached, pumping will carry on until such a state is reached or as instructed by the engineer; the minimum test period will be 7 days.

7.1.5. Phase 1

(1) Pump sunk to -16.05 mPD

(2) Commencement of pumping test (first stage)

(3) Lower down water table level to -9.3 mPD

(4) Permanent instrumentation monitoring through observation wells and piezometers

(5) If an excessive drawdown of the ground water level occurs (GWT level below -0.5 mPD) outside the diaphragm wall, a recharge well corrective system will be operated resulting in the failure of the pumping test

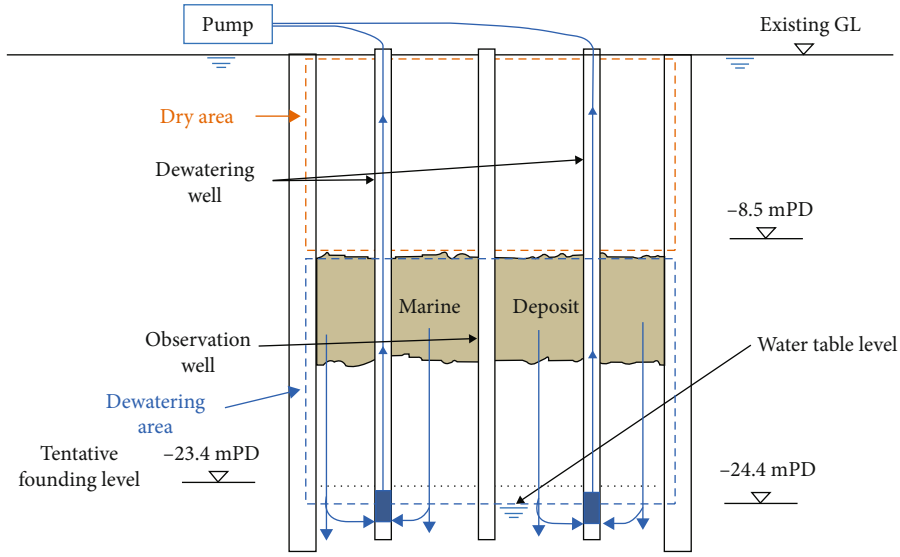

Figure 16: Pumping tests, stage 2.

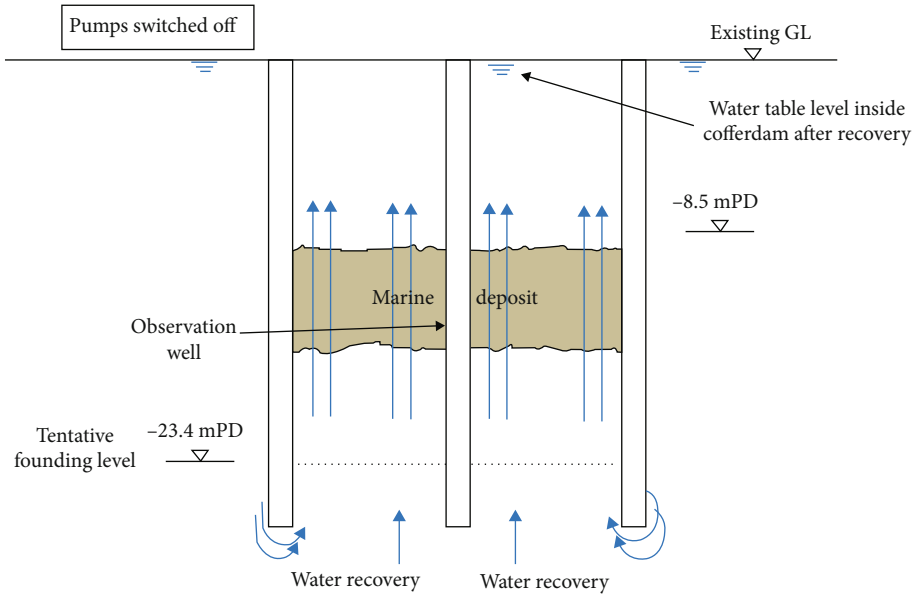

Figure 17: Recovery phase.

(6) After achievement of steady state at -9.3 mPD, the phase 2 pumping test can commence

7.1.6. Phase 2

(1) The pump sunk to the required level depending on the location (see table above)

(2) Commencement of pumping test (second stage)

(3) Lower down water table level to -24.4 mPD

(4) Permanent instrumentation monitoring through observation wells and piezometers

(5) If an excessive drawdown of ground water level occurs (GWT level below -0.5 mPD) outside the diaphragm wall, a recharge well corrective system will be operated resulting in the failure of the pumping test

(6) After the achievement of steady state at -24.4 mPD, the recovery phase can commence

7.1.7. Recovery Phase. During the recovery phase, all pumps will be switched off. Hence, the water level will slowly increase inside the cofferdam until reaching its initial level or after 2 days, whichever is sooner. During this phase, the monitoring will carry on until the water levels in both the observation wells and the piezometers have recovered their initial levels. The engineer will be notified prior to termination of taking readings.

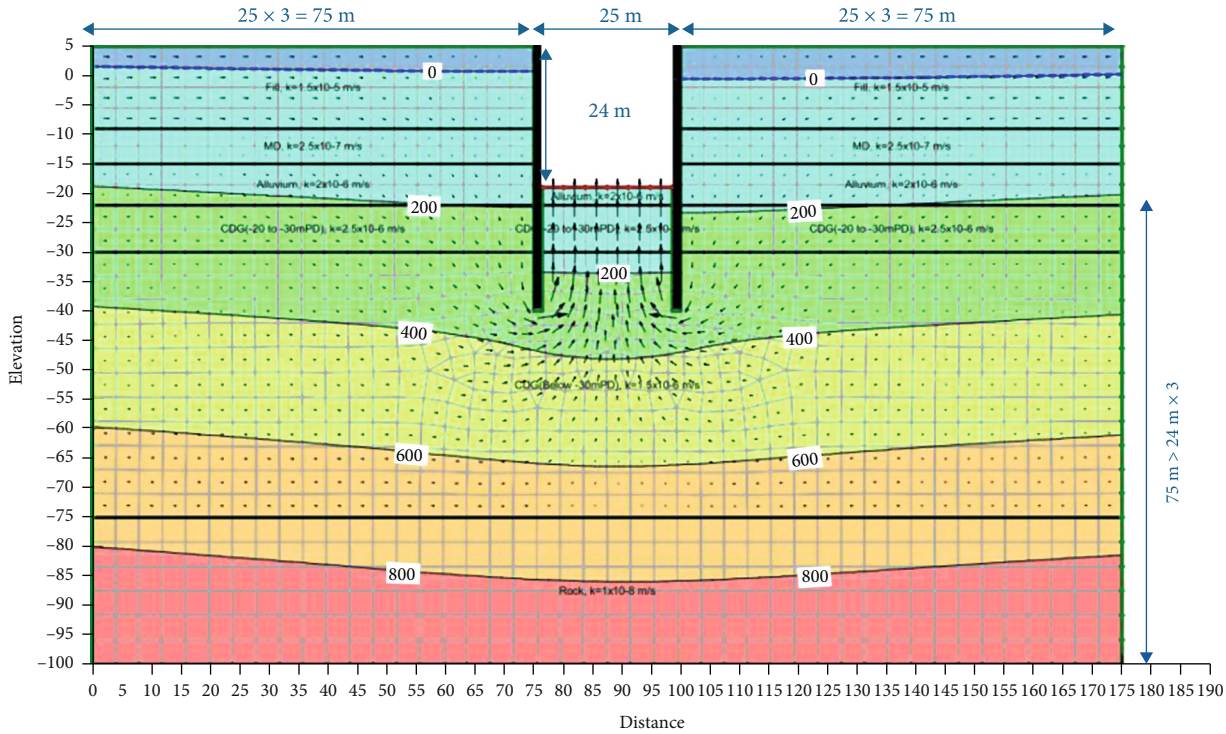

Figure 18: Seepage analysis for the West Kowloon Reclamation.

7.1.8. Monitoring Plan during Pumping Test. As explained above, the contractor has installed several monitoring points. Each monitoring instrument intends to monitor the following:

(1) Any movement of existing structures adjacent to the 811A project

(2) Any undue ground settlement

(3) Any nonstandard ground water table level outside the cofferdam

Different monitoring phases will be encountered during the pumping tests: before pumping tests, the contractor will monitor water levels of dewatering wells and observation wells inside the cofferdam. Those readings will form the base set of initial data for the pumping test.

Different kinds of monitoring equipment were installed and took the initial reading prior to commencement of the pumping test. During the pumping test, these monitoring points should be monitored daily; if any excessive movement was found according to the allowable movement, the pumping test should be ceased immediately.

7.2. Determination of Permeabilities by the Dewatering Tests. The pumping test results are measured and compared with the numerical results from Flac3D seepage analysis. The permeabilities of different types of soils are adjusted until the measured results match well with the numerical results (see Figure 18). The in situ measured permeabilities are then used for the future analysis and design of the construction works. This approach is also used for the West Kowloon reclamation project in Hong Kong (another large scale project in Hong Kong). By comparing the results of 27 trial cases with different combinations of permeability for each layer of soil with the field dewatering test, the permeability for each layer of soil as shown in Table 7 was found to be most appropriate with the result of the field dewatering tests. Based on Table 7, the seepage analysis for the West Kowloon reclamation project is carried out as shown in Figure 18.

Table 7: Permeabilities of different types of soil from the dewatering tests.

Soil	Permeability
Fill	1.5×10^{-5}
Marine deposit	2.5×10^{-7}
Alluvium	4×10^{-6}
CDG (-20 to -30 mPD)	1.4×10^{-6}
CDG (below -30 mPD)	8.3×10^{-7}
Rock	1×10^{-8}

8. Discussions and Conclusion

In this paper, the authors have discussed various methods that are used for the analysis of the seepage problem. Based on the use of various numerical methods and computer programs, the authors view that the finite element method is the most versatile method among all, while the analytical method is actually sufficient for normal engineering problems. The authors have also collected several cases from different

projects in Hong Kong, and the importance of a good seepage analysis is well recognized by many engineers.

Based on the present study, some conclusion can be drawn:

(1) Based on the analytical formulae, it can be observed that the existence of an impermeable boundary at the bottom of the excavation will slightly increase the water pressure. This effect is however small in general, and the assumption of a rock boundary at infinity is actually sufficient for normal engineering design

(2) Based on the Hillwood Road project, it is established that the free surface flow is important for the seepage problem in loose soil. This is further supported by the observations of large drawdown of the water table for the Sheung Wan and Wanchai MTR Concourses and major ground settlement due to change of pore water pressure outside the diaphragm wall, which is very important for the construction of deep excavations in loose soils

(3) The net water pressure on a retaining wall as shown in Figure 11 is not appreciated by many engineers or researchers. The actual net water pressure which is shown by the blue line in Figure 11 is virtually never addressed by the engineers or researchers, but this is actually observed by Cheng in some deep excavation projects in Hong Kong. The results in this paper also reflect the problems in nearly all the existing textbooks which have not clearly considered the actual water pressure in a deep excavation construction

(4) The two large scale field tests have illustrated the importance of obtaining the true permeabilities of soils against the use of unreliable laboratory tests. The authors have also illustrated the possibility of carrying out back analysis to obtain the permeability for a proper seepage analysis for the coming construction works

Data Availability

The data used to support the findings of this study are available from the corresponding authors upon request.

Conflicts of Interest

The authors declare that they have no conflicts of interest.

Acknowledgments

The work described in this paper was supported by the State Key Program of the National Natural Science Foundation of China (Grant No. U1802243), National Natural Science Foundation of China (Grant No. 51778313), and Cooperative Innovation Center of Engineering Construction and Safety in Shandong Blue Economic Zone.

References

[1] C. Zhu, Z. H. Yan, Y. Lin, F. Xiong, and Z. Tao, "Design and application of a monitoring system for a deep railway foundation pit project," *IEEE Access*, vol. 7, pp. 107591–107601, 2019.

[2] H. Y. Pan, D. W. Yin, N. Jiang, and Z. G. Xia, "Crack initiation behaviors of granite specimens containing crossing-double-flaws with different lengths under uniaxial loading," *Advances in Civil Engineering*, vol. 2020, Article ID 8871335, 13 pages, 2020.

[3] Y. Wang, B. Zhang, S. H. Gao, and C. H. Li, "Investigation on the effect of freeze-thaw on fracture mode classification in marble subjected to multi-level cyclic loads," *Theoretical and Applied Fracture Mechanics*, vol. 111, p. 102847, 2020.

[4] C. Zhu, M. C. He, M. Karakus, X. B. Cui, and Z. G. Tao, "Investigating toppling failure mechanism of anti-dip layered slope due to excavation by physical modelling," *Rock Mechanics and Rock Engineering*, vol. 53, no. 11, pp. 5029–5050, 2020.

[5] Z. Tao, C. Zhu, X. Zheng, and M. He, "Slope stability evaluation and monitoring of Tonglushan ancient copper mine relics," *Advances in Mechanical Engineering*, vol. 10, no. 8, Article ID 168781401879170, 2018.

[6] Y. M. Cheng, C. W. Law, and L. L. Liu, *Foundation Analysis, Design and Construction*, CRC Press, 2021.

[7] C. Zhu, X. D. Xu, and W. R. Liu, "Softening damage analysis of gypsum rock with water immersion time based on laboratory experiment," *IEEE Access*, vol. 7, pp. 125575–125585, 2019.

[8] Z. Li, H. Liu, Z. Dun, L. Ren, and J. Fang, "Grouting effect on rock fracture using shear and seepage assessment," *Construction and Building Materials*, vol. 242, p. 118131, 2020.

[9] Z. Li, S. Liu, W. Ren, J. Fang, Q. Zhu, and Z. Dun, "Multiscale laboratory study and numerical analysis of water-weakening effect on shale," *Advances in Materials Science and Engineering*, vol. 2020, Article ID 5263431, 14 pages, 2020.

[10] M. I. Haque, *Mechanics of Groundwater in Porous Media*, CRC Press, 2015.

[11] G. Kovacs, *Seepage Hydraulics*, Elsevier, 1981.

[12] F. D. Smedt and W. Ziji, *Two- and Three-Dimensional Flow of Groundwater*, CRC Press, 2018.

[13] O. D. L. Strack, *Analytical Groundwater Mechanics*, Cambridge University Press, 2017.

[14] Q. Meng, H. Wang, M. Cai, W. Xu, X. Zhuang, and T. Rabczuk, "Three-dimensional mesoscale computational modeling of soil-rock mixtures with concave particles," *Engineering Geology*, vol. 277, article 105802, 2020.

[15] L. L. Yang, W. Y. Xu, Q. X. Meng, and R. B. Wang, "Investigation on jointed rock strength based on fractal theory," *Journal of Central South University*, vol. 24, no. 7, pp. 1619–1626, 2017.

[16] Q. X. Meng, L. Yan, Y. L. Chen, and Q. Zhang, "Generation of numerical models of anisotropic columnar jointed rock mass using modified centroidal voronoi diagrams," *Symmetry*, vol. 10, no. 11, p. 618, 2018.

[17] Q. X. Meng and W. Wang, "A novel closed-form solution for circular openings in generalized Hoek-Brown media," *Mathematical Problems in Engineering*, vol. 2014, no. 2, Article ID 870835, 7 pages, 2014.

[18] Y. Fukuo and I. Kaihotsu, "A theoretical analysis of seepage flow of the confined groundwater into the lake bottom with a gentle slope," *Water Resources Research*, vol. 24, no. 11, pp. 1949–1953, 1988.

[19] P. Bettess, "Infinite element," *International journal for numerical methods in engineering*, vol. 11, no. 1, pp. 53–64, 1977.

[20] Y. Honjo and G. Pokharel, "Application of infinite elements to seepage analysis in geotechnical perspective," *Soils and Foundations*, vol. 33, no. 1, pp. 23–39, 1993.

[21] Y. M. Cheng, "The use of infinite element," *Computers and Geotechnics*, vol. 18, no. 1, pp. 65–70, 1996.

[22] F. Azizi, *Applied Analyses in Geotechnics*, E & FN Spoon, New York, 2000.

[23] HKIE, *An Explanatory Handbook to Code of Practice for Foundations 2017*, HKIE, Hong Kong, 2017.

[24] Z. L. Li, Z. H. Qiao, and T. Tang, "Numerical Solution of Differential Equations," in *Introduction to finite difference and finite element method*, Cambridge University Press, 2018.

[25] I. M. Smith, D. V. Griffiths, and L. Margetts, *Programming the Finite Element Method*, John Wiley & Sons, 5th edition, 2014.

[26] M. Asadzadeh, *An Introduction to the Finite Element Method for Differential Equations*, John Wiley & Sons, 2021.

[27] P. M. Cashman and M. Preene, *Groundwater Lowering in Construction*, CRC Press, 3rd edition, 2021.

[28] J. P. Powers, A. B. Corwin, P. C. Schmall, W. E. Kaeck, and C. J. Herridge, Eds., *Construction Dewatering and Groundwater Control*, John Wiley & Sons, 2007.

[29] R. J. Sterrett, *Ground Water and Wells*, John Screens, 3rd edition, 2007.

[30] C. Baiocchi, V. Comincioli, E. Magenes, and G. A. Pozzi, "Free boundary problems in fluid flow through porous media: existence and uniqueness theorems," *Annali di Matematica Pura ed Applicata*, vol. 97, pp. 1–82, 1973.

[31] S. A. Ridlon, "Modelling guidelines," *Finite Element Idealization for Linear Elastic Static and Dynamic Analysis of Structures in Engineering Practice*, pp. 212–272, 1987.

[32] Y. M. Cheng and Y. Tsui, "An efficient method for the free surface seepage flow problems," *Computers and Geotechnics*, vol. 15, no. 1, pp. 47–62, 1993.

[33] C. Y. Ou, *Deep Excavation*, Taylor & Francis, 2006.